Rheology and Shear Orientation of a Nematic Liquid Crystalline Side-Group Polymer with Laterally Attached Mesogenic Units

Jörg Berghausen, Joachim Fuchs,† and Walter Richtering*

Albert-Ludwigs-Universtität Freiburg i. Br., Institut für Makromolekulare Chemie, Stefan-Meier-Strasse 31, D-79104 Freiburg, Germany

Received March 28, 1997; Revised Manuscript Received September 3, 1997[⊗]

ABSTRACT: The shear orientation of a nematic side-group liquid crystalline polymer (SG-LCP) with side-on fixed mesogenic units was investigated by means of rheo-birefringence and rheo-small angle light scattering. Rheological properties of the polymer depend on molecular weight. Macroscopically aligned samples were obtained in creep experiments, but the orientation was destroyed by oscillatory shear flow. The shear modulus of a low molar mass sample in the nematic and isotropic phase superposed to a common master curve. The low-frequency modulus of a high molar mass sample, however, decreased at the phase transition, and time−temperature superposition was not possible. Preshearing led to a further decrease of the modulus. Rheo-birefringence measurements revealed a clear influence of molar mass on both the final value and the orientation state after cessation of shear. Rheo-small angle light scattering also showed a strong influence of molecular weight. In polarizing microscopy, a banded texture was observed with a high molar mass sample. The polymer showed a pronounced pretransitional behavior. This regime slightly above the phase transition revealed a strong decoupling between the polymer backbone and the mesogens. Different relaxation times were found for creep recovery and birefringence, respectively.

1. Introduction

Liquid crystalline materials are characterized by a long range orientational order between the mesogenic groups. In samples of macroscopic size, the order will not be spatially homogeneous and defects give rise to a texture that can be observed in a polarizing microscope. Rheological properties of liquid crystalline polymers (LCPs) are rather complex due to the anisotropy of the material. Furthermore, the shear flow itself is known to alter the structure of the material under investigation. Therefore, shear-induced structural changes should be monitored simultaneously with the rheological experiment and various techniques have been developed for that purpose.[1,2]

Much work has been done on the shear orientation of lyotropic liquid crystalline phases of stiff macromolecules, and it has been postulated by Onogi and Asada[3] that liquid crystalline polymers exhibit three regions of steady shear flow: region I is classified by shear thinning at low shear rates and the flow behavior is dominated by defects,[4] region II has a viscosity plateau and texture refinement,[5] and region III has a second shear-thinning region where a monodomain is reached at higher shear rates. Theoretical descriptions usually apply rigid rod models,[4,6,7] and features such as flow alignment or tumbling of the director are discussed. A mesoscopic approach was given by Larson and Doi[8] and predicts the influence of shear rate on the domain size. This flow behavior was observed in lyotropic as well as in thermotropic LCPs.[9−14]

However, there are two major classes of thermotropic LCPs: (i) in main-chain LCPs the mesogenic groups are part of the polymer main chain, whereas (ii) in side-group liquid crystalline polymers (SG-LCP), the mesogens are part of the side group that is connected to the polymer backbone by a flexible spacer. Usually, the backbone of SG-LCPs is rather flexible and therefore it is not clear whether rigid rod models are appropriate to describe flow properties of such LCPs.

Much less is known about rheological properties of SG-LCPs as compared to main-chain LCPs and most studies only used polymers with a rather low degree of polymerization.[15−19] The decoupling between the rigid mesogenic group and the flexible polymer backbone leads to a complex flow behavior, and the final properties of processed liquid crystalline polymers depend on the microstructure developed during processing. For widespread use of this class of materials it is important to know more about the influence of microstructure on the molecular, the mesoscopic, and the macroscopic level.

Because of the intrinsically anisotropic properties of the mesogenic units, flow should be a powerful means of producing shear orientation, as known from main-chain liquid crystalline polymers.[20] From earlier investigations of the rheology of SG-LCPs with an end-on fixed mesogenic unit[15] it was concluded that the rheological behavior of nematic SG-LCPs is dominated by the flexible backbone. It was deduced that the liquid crystalline (LC) character should not influence the viscoelasticity of the SG-LCP and therefore, shear flow was assumed to be not powerful in aligning this type of liquid crystalline polymer.

However, a few years ago, Kannan et al.[21] showed that SG-LCPs with *linearly* (**end-on**) fixed mesogenic groups can be aligned by large amplitude oscillatory shear deformation. The orientation can be fixed by cooling into the glassy state. Highly oriented nematic SG-LCPs have attracted interest due to their use as nonlinear optical materials, optical data storage media, and stress sensors.[22]

Kornfield and co-workers[21,23] also observed that the shear alignment affected the linear viscoleastic properties of the material when the molecular weight was sufficiently high so that entanglements were present. Then shear orientation led to a decrease of storage and loss modulus in the low-frequency range.

In the present work we investigated the influence of shear on a SG-LCP with *laterally* (**side-on**) fixed mesogenic groups.[24,25] The polymer exhibits a sharp

* To whom correspondence should be sent. E-mail: rich@ruf.uni-freiburg.de.
† Present address: Bohlin Instruments, Mühlacker, Germany.
⊗ Abstract published in *Advance ACS Abstracts,* November 1, 1997.

S0024-9297(97)00430-0 CCC: $14.00

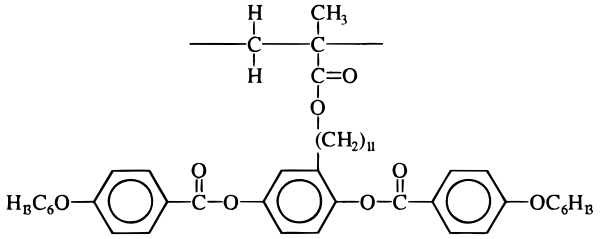

Figure 1. Repeating unit of the SG-LCP.

Table 1. Comparison of the Different Polymer Samples Used in This Study[a]

sample	$10^5 M_w$ (g/mol)	DP_w	T_g (°C)	T_{ni} (°C)
SG-LCP-1	1.68	222	4	59.5
SG-LCP-2	18.9	2500	6	58.5

[a] Molecular weights were detected by static light scattering, and transition temperatures were measured by differential scanning calorimetry (DSC).

phase transition from the nematic to the isotropic phase within a remarkably small region of ca. 1 K. In addition, the phase transition temperature is quite low and therefore experimental studies can be performed at convenient temperatures. The same systems have been used by Finkelmann and co-workers to investigate properties of LC elastomers.[26]

The repeating unit of the nematic side-group liquid crystalline polymer used in this study is shown in Figure 1 and consists of a polymethacrylate backbone and a hydroquinone bis(benzoate) mesogen coupled *laterally* to a long spacer of 11 methylene units. Experiments were carried out on two samples with different molecular weights. Table 1 summarizes the molecular weight, M_w, the degree of polymerization, DP_w, the glass transition temperature, T_g, and the nematic to isotropic phase transition temperature, T_{ni}, of the two samples.

It is known that the liquid crystalline order of the mesogenic side groups also affects the configuration of the polymer backbone. A prolate shape was often found with side-on polymers. However, the anisotropy of the macromolecule is less pronounced when a long spacer and long aliphatic tails are present, as is the case of the polymers used here.[27] Consequently the mesogenic groups are strongly decoupled from the polymer backbone and one motivation for this study was to find out whether or not shear orientation is possible despite the long spacer.

2. Experimental Part

Synthesis and purification of the polymers were performed as described by Hessel et al.[25]

Rheological measurements were performed using a Bohlin CS-10 constant stress rheometer equipped with parallel plates of 2 cm diameter and a sample thickness of 0.5 mm. Simple shear and oscillatory shear were used.

Shear orientation was monitored by turbidity, birefringence, and small angle light scattering. For rheo-optical studies the Bohlin CS-10 rheometer was equipped with a quartz glass plate and plate shear geometry (4 cm diameter). The sample thickness used in these experiments was 0.2 mm. Rheological data were the same as for the thicker samples. For birefringence and light scattering experiments the incident laser beam of a He−Ne laser ($\lambda_0 = 632.8$ nm) passed through the sample along the direction of the velocity gradient and perpendicular to the flow direction. The retardance was determined using the method described by Lim and Ho.[28] The actual experimental setup is given elsewhere.[29] In order to obtain the absolute value of birefringence, the number of orders has to be determined. This could be achieved either by shearing the sample during cooling from the isotropic to the nematic phase or by heating a shear-aligned nematic sample to the isotropic phase while simultaneously keeping track of the number of orders. The turbidity of the samples was described with the transmitted intensity, which was normalized by the transmission of the sample in the isotropic phase.

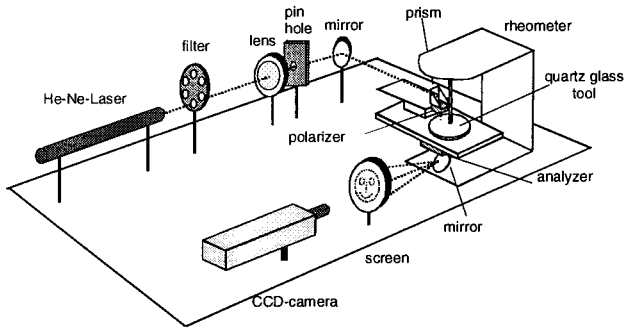

Figure 2. Small-angle light scattering apparatus.

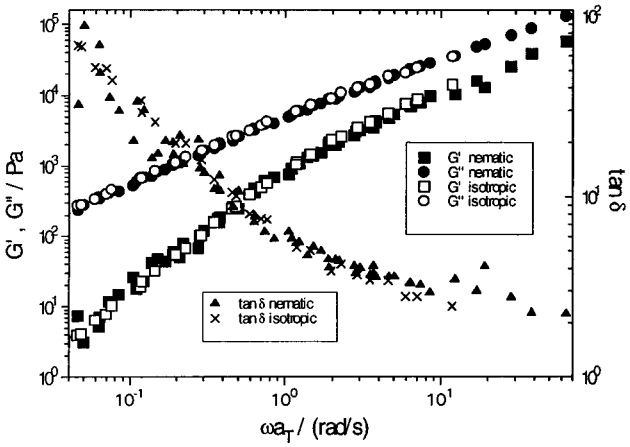

Figure 3. Master curve of storage and loss modulus ($T_0 = 55$ °C) for SG-LCP-1.

Figure 2 shows the homemade apparatus used for rheo-small angle light scattering (SALS). Only depolarized H_v-SALS was investigated in this study. Here, the primary beam was vertically polarized along the flow direction and the depolarized scattered intensity was detected. The accessible q-range was 1.62 μm^{-1} horizontally and 1.23 μm^{-1} vertically.

Prior to all experiments the polymer samples were heated into the isotropic phase and held there for at least 15 min. To make sure that the samples did not degrade during experiments, the weight average molar mass was measured by static light scattering from dilute solutions before and after the rheo-optical experiments. No change in molar mass could be found within experimental error. Solution properties of the SG-LCPs and the refractive index increment have been reported elsewhere.[30]

3. Results

3.1. Rheological Experiments. The low molar mass sample SG-LCP-1 revealed rather simple rheological properties. Steady shear flow was easily reached and the viscosity was independent of shear rate in the whole temperature range (40−80 °C). A discontinuity of the viscosity at the isotropic to nematic phase transition was not observed.

Dynamic-mechanical experiments were performed in the same temperature range. A common master curve could be obtained by time−temperature superposition for both phases and is displayed in Figure 3.

The high molar mass sample SG-LCP-2 showed different behavior. Steady shear flow was not reached within reasonable creep times, thus the shear viscosity

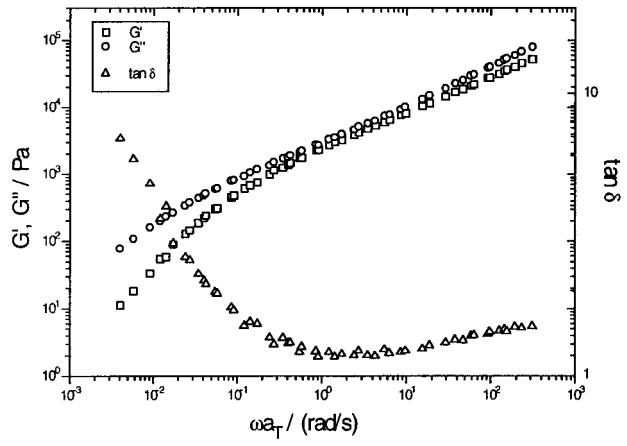

Figure 4. Master curve of storage and loss modulus ($T_0 = 55$ °C) for SG-LCP-2 in the isotropic phase.

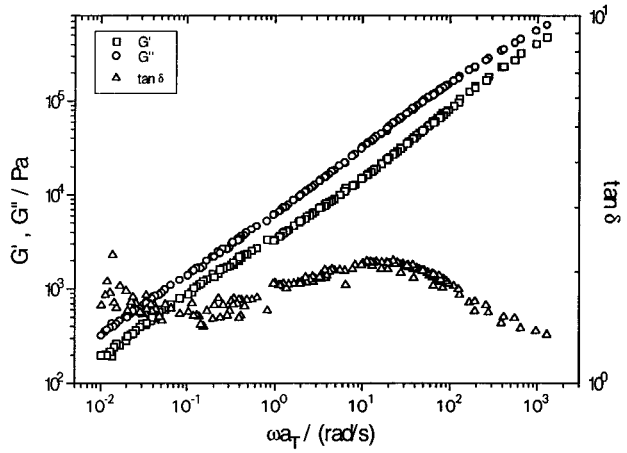

Figure 5. Master curve of storage and loss modulus ($T_0 = 55$ °C) of SG-LCP-2 in the nematic phase.

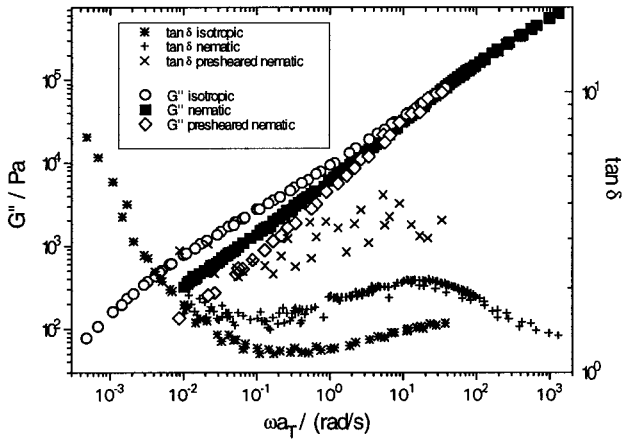

Figure 6. Master curves of loss modulus for SG-LCP-2 in the isotropic, nematic, and presheared nematic phase ($T_0 = 55$ °C).

was not determined. Creep recovery was found in creep experiments. Different behavior was also observed in low amplitude oscillatory shear experiments. A common master curve for the isotropic and the nematic phase could ***not*** be obtained. Figures 4 and 5 show master curves for the isotropic and the nematic phase, respectively. In the nematic phase, storage and loss moduli could be changed by preshearing the sample.

Figure 6 gives a comparison of the loss modulus G'' in the isotropic, nematic (polydomain), and the presheared nematic phase. The three curves could be superposed at high frequencies. However, the tan δ

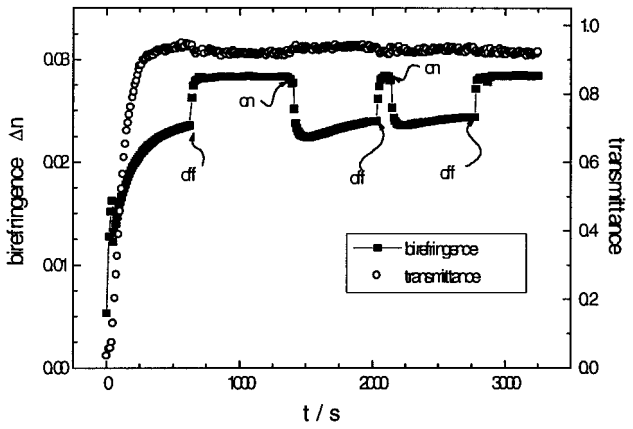

Figure 7. Behavior of SG-LCP-2 in a creep experiment ($\sigma =$ 590 Pa, $T = 55$ °C) starting with a polydomain. Arrows indicate when the shear stress was switched on and off.

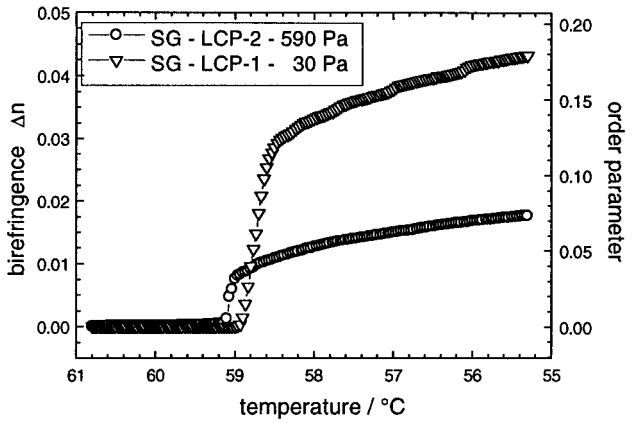

Figure 8. Birefringence and order parameter measured during cooling from the isotropic into the nematic phase under shear.

curves did not superpose; i.e., the relaxation spectra of isotropic, nematic (polydomain), and aligned nematic were different in the whole accessible frequency range. The moduli decreased with increasing mesophase order, i.e., from isotropic to nematic to presheared nematic. The decrease of the storage modulus G' was more pronounced as compared to G''.

3.2. Birefringence. Flow birefringence measurements were performed in order to obtain information on shear orientation. When the sample was cooled from the isotropic to the nematic phase, a turbid, polydomain specimen was obtained. The sample became optically transparent during shear; see Figure 7. In a second set of experiments, the sample was slowly cooled into the nematic phase and sheared simultaneously. The sample stayed transparent during the phase transition when the applied stress was sufficiently high so birefringence could be determined. Because of the temperature gradient within the sample, the phase transition did not occur exactly at the same temperature as determined by DSC. Examples are shown in Figure 8.

The final birefringence value was independent of the applied shear stress for both samples, but higher values were obtained from the sample with lower molar mass SG-LCP-1, namely $\Delta n = 0.055 \pm 0.003$ for SG-LCP-1 and $\Delta n = 0.022 \pm 0.002$ for SG-LCP-2. Lower Δn values were found with thicker samples.

The two samples showed different behaviors after cessation of shear. With the low molar mass sample SG-LCP-1 a very slight decrease of transparency and birefringence was observed. The high molar mass

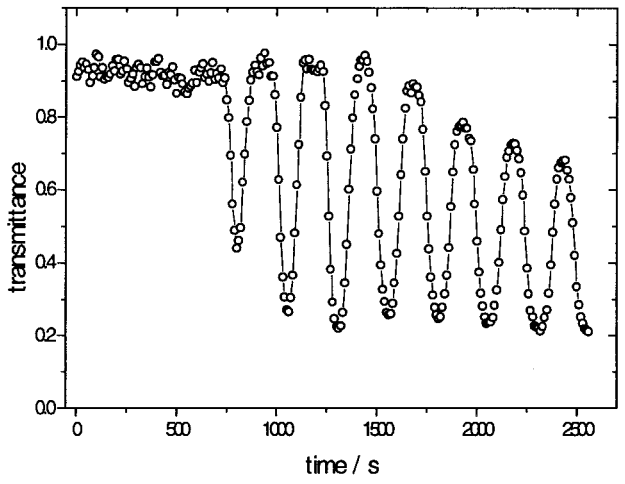

Figure 9. Transmittance of a presheared SG-LCP-2 sample in an oscillatory shear experiment at a frequency of 0.004 Hz (σ = 50 Pa, T = 55 °C). The polymer has been aligned in a creep experiment with σ = 590 Pa for 1000 s. The line is a guide to the eye.

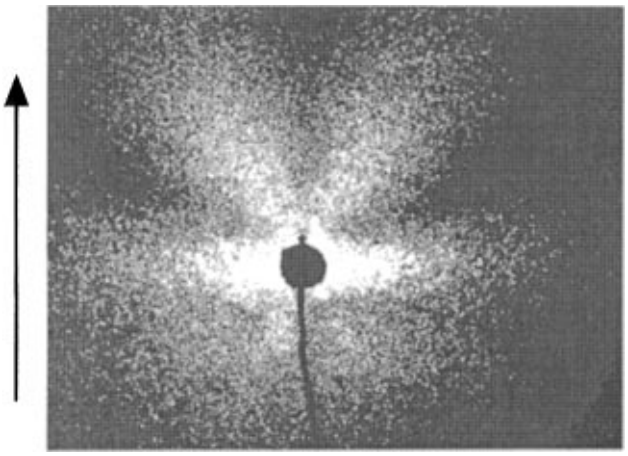

Figure 10. H_V SALS pattern of the low molar mass sample SG-LCP-1 under shear. The arrow indicates the flow direction.

sample, however, showed an increase of Δn after cessation of shear; see Figure 7.

Large amplitude oscillatory shear experiments were also employed. However, optically transparent samples could not be obtained with oscillatory shear. Samples aligned in creep experiments became turbid again when oscillatory shear was applied afterward, as shown in Figure 9. The sample was oriented in a creep experiment and became transparent and highly birefringent. Then oscillatory shear with σ = 50 Pa was applied with a frequency of 0.004 Hz. Figure 9 shows that the turbidity changed with the oscillatory cycle and an overall decrease of transmitted intensity was found.

3.3. Rheo-Small Angle Light Scattering. Depolarized (H_v) SALS patterns were also recorded during creep experiments. Figure 10 shows the scattering pattern observed from the low molar mass sample under shear. It consisted of a streak perpendicular to the flow direction and a four-lobe pattern with an intensity anisotropy. After cessation of shear, the scattering pattern became smeared and eventually isotropic.

Figure 11 shows the H_v SALS picture of the high molar mass sample as a function of creep time. An elliptical pattern was observed that was tilted with respect to the flow direction. The streak became sharper with increasing creep time and was eventually adjusted perpendicular to the flow direction; simultaneously, the scattering intensity decreased. During creep recovery, the scattering pattern became isotropic.

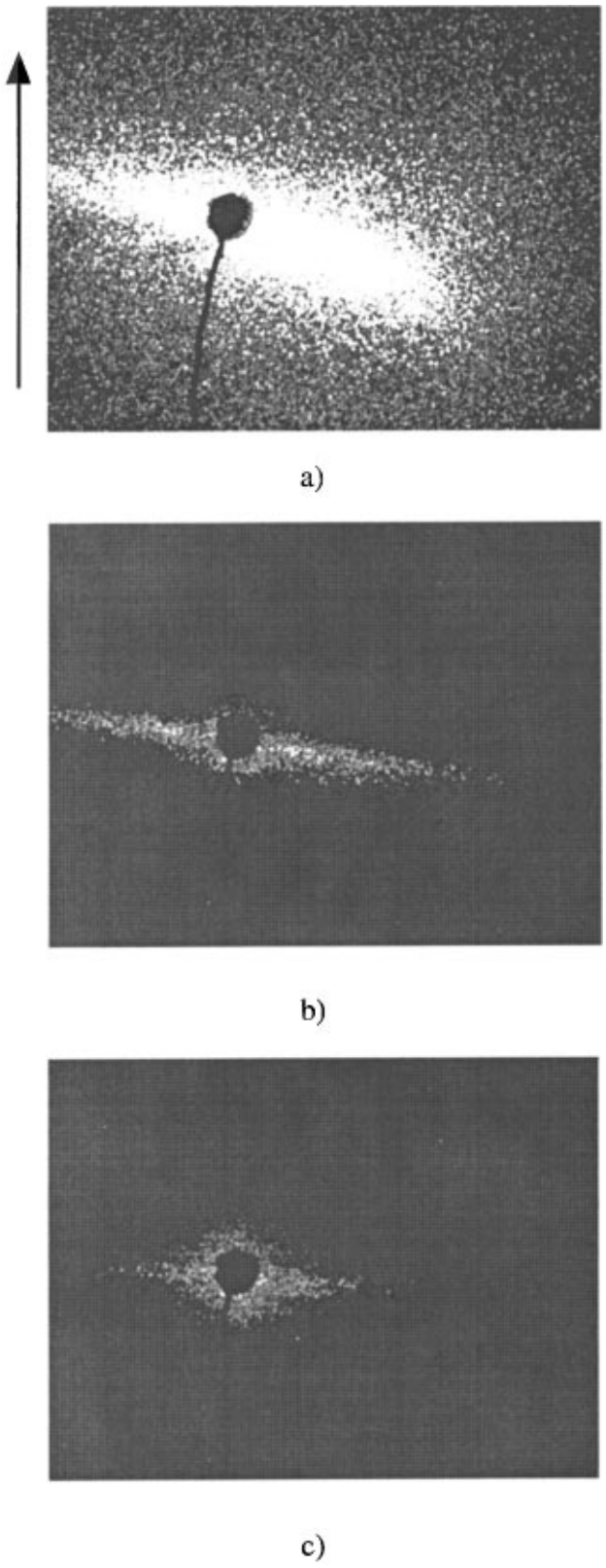

Figure 11. H_V SALS pattern of the high molar mass sample SG-LCP-2 as a function of creep time (σ = 590 Pa): (a) 50 s; (b) 600 s, (c) 1000 s. The arrow indicates the flow direction.

3.4. Pretransitional Regime. Flow birefringence experiments have also been performed at temperatures slightly above the phase transition. Figures 12 and 13 show the stress and temperature dependence of shear-induced birefringence for both samples. Higher Δn

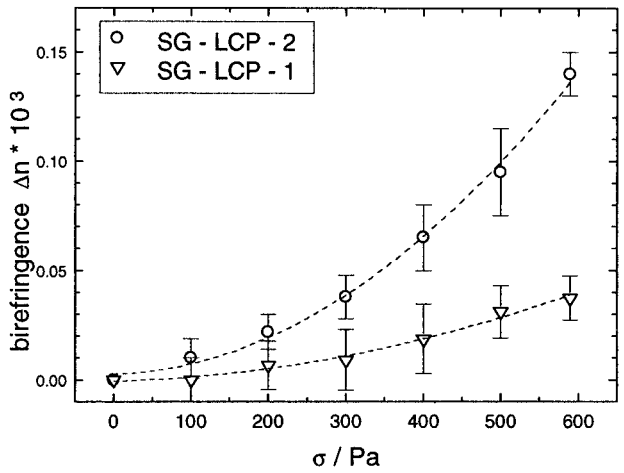

Figure 12. Flow birefringence in the pretransitional regime (T = 60.5 °C) as a function of shear stress. The dashed lines represent second-order fits.

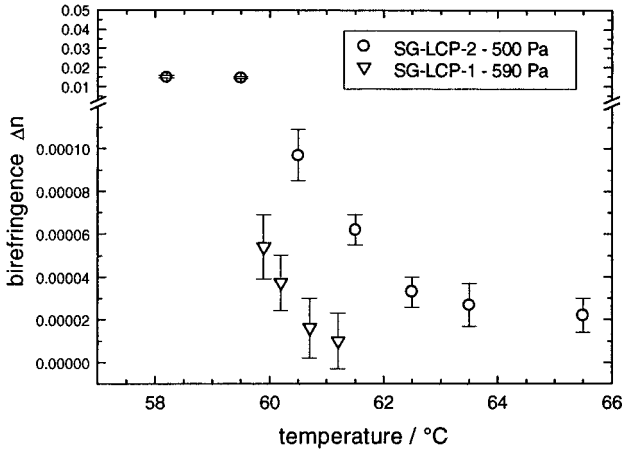

Figure 13. Flow birefringence in the pretransitional regime as a function of temperature.

values were obtained with the high molar mass sample, in contrast to the results obtained in the nematic phase.

4. Discussion

In the following we wish to discuss viscoelastic properties and shear orientation of the SG-LCP with laterally attached mesogenic groups. The results will be compared with the behavior of other LCPs and especially with SG-LCPs studied in detail by Kornfield and co-workers.[21,23]

First we wish to discuss the pretransitional behavior. Figures 12 and 13 show that shear flow increased the birefringence. The stress dependence in Figure 12 could be fitted to a second-order polynomial; thus the same dependence was observed, as is known from LC elastomers and as was predicted theoretically.[31] Of course the effect of shear flow is much smaller as compared to stretching a cross-linked sample. Schätzle et al.[26] stretched LC elastomers prepared from the same monomer. They were able to change the phase transition from first to second order, whereas the shear flow used in our study could not alter the type of phase transition.

The rheological properties of the **low molar mass sample SG-LCP-1** were rather simple: steady shear flow was easily reached, and no discontinuity was observed at the isotropic to nematic phase transition. Thus the temperature dependence of viscosity is different from low molar mass LC and main chain LCPs.[20,32]

Table 2. Activation Energies (kJ/mol) Obtained from Melt Viscosity and Shift Factors

	SG-LCP-1		SG-LCP-2
	viscosity	shift factor	shift factor
isotropic phase	90.0 ± 1.3	87.9 ± 2.4	86.5 ± 6.3
pretransitional regime	103.1 ± 2.7	106.1 ± 1.7	103.6 ± 5.9
nematic phase	130.0 ± 2.3	136.0 ± 1.7	134.2 ± 2.4

A single master curve for G' and G'' was obtained for both phases, and no creep recovery was observed. The temperature dependences of viscosity and shift factors were of Arrhenius type and the activation energies are summarized in Table 2. The activation energies are similar to the values obtained by Zentel and Wu[15] with end-on SG-LCP. Table 2 gives the results for both samples, and obviously, there is no influence of chain length.

Figure 3 shows that a single master curve was found for G' and G'' for both phases. Obviously, the relaxation spectrum was not influenced by the phase transition, indicating that rheological properties are dominated by the polymer backbone. After cessation of shear no strain recovery was found. This behavior is different from rigid rod LCPs, which are characterized by large recoverable strains.[33]

In the nematic phase the polydomain sample is easily aligned by shear flow. Large amplitude oscillatory shear, however, gave no shear orientation, thus the side-on SG-LCPs are different from end-on SG-LCPs. This might be due to the different orientation of the mesogenic group. In the case of the end-on polymers studied by Kornfield and co-workers the mesogenic groups were oriented perpendicular to the flow direction and a reversal of the shear direction does not influence the orientation. In our case, however, the mesogenic groups were aligned along the flow direction and obviously flow reversal strongly affected the orientation.

Since the optical properties of the investigated side-on SG-LCP were studied by Hessel,[34] the order parameter can be calculated from the birefringence by assuming that the optically transparent sample is close to a monodomain. The order parameter is shown in Figure 8 and was significantly smaller as compared to values obtained by Schätzle et al. for stretched SG-LCP elastomers.[26] The lower Δn values can be caused by the different type of deformation, shear, and elongation, respectively.[17] Lower Δn values might also be explained by an increased Leslie angle. Furthermore, the small birefringence could be due to a nonhomogeneous orientation. SALS experiments discussed below showed the existence of defects in the SG-LCPs under shear and a nonuniform mesogen orientation could also be responsible for the small Δn values. Since viscosity and order parameter were independent of shear rate (in the range available for this study), the SG-LCP-1 resembled region II flow behavior in the model of rigid rod LCPs described by Onogi and Asada.[3]

The H_v-SALS pattern shown in Figure 10 also demonstrates similarities of the SG-LCP with other LCPs. The same scattering pattern has been observed before from nematic solutions of stiff macromolecules.[35−37] The streak perpendicular to the flow direction is related to stretched disclination lines. These disclination lines could be directly observed by shearing the sample under a polarization microscope. The origin of the four-lobe pattern is not yet clear. A possible interpretation was given by Vermant et al. who related the four-lobe pattern to orientation fluctuations and distortions of the director field.[37] We wish to note that the intensity

anisotropy of the four lobes has also been observed in other systems and again is nicely described by Vermant.

The sample with **high molar mass SG-LCP-2** revealed a more complicated behavior. Steady shear flow was not reached within the creep times employed in this study. The birefringence, however, reached a constant value. This indicates again that rheological properties, dominated by the backbone, and the orientation of the mesogenic groups are decoupled. However, the Δn values were smaller as compared to the low molar mass sample. Apparently, the resistance of the backbone against deformation also affects the degree of orientation of the mesogens.

An elliptical scattering pattern was observed in depolarized SALS, which sharpened with creep time. The angle of the streak with respect to the vorticity direction decreased with time (see Figure 11), and this angle could be correlated with the curvature of the creep compliance. The streak corresponds to stretched disclination lines, as discussed above. Apparently, the alignment of disclination lines depends on the viscous properties of the sample, which are dominated by the polymer backbone.

Turbidity, SALS, and birefringence demonstrate that the structure of the material was strongly influenced by shear flow with both samples. However, SALS and flow birefringence showed that the mesogen orientation was not perfect. Although shear flow produced a highly transparent sample, transparency should not be interpreted as proof of the formation of a monodomain.

A further difference between the two samples was the relaxation behavior after cessation of shear. Creep recovery was only observed with the high molar mass sample SG-LCP-2. However, the absolute value of the recovered strain was rather small; i.e., the behavior in creep recovery was similar to that of conventional polymeric materials and differed from that of rigid rod LCPs.[33,38,39] This again demonstrates that the influence of the polymer backbone on rheological properties was higher than the influence of the nematic order of the side groups.

The decoupling of rheological properties dominated by the backbone and optical properties dominated by the mesogens can be deduced also from the different relaxation times after cessation of shear. Relaxation times of birefringence $\tau(\Delta n)$ and strain recovery $\tau(\gamma_{rec})$ were calculated in the pretransitional region and the nematic phase for SG-LCP-2. In both cases the relaxation behavior was not single exponential. The relaxation process was fitted to a stretched exponential (Kohlrausch−Williams−Watt function):[40−42]

$$g(t) = y + a\mathrm{e}^{(-t/t_1)^{\beta}} \tag{1}$$

The average relaxation time τ is given by

$$\tau = \frac{t_1}{\beta}\Gamma\left(\frac{1}{\beta}\right) \tag{2}$$

where $\Gamma(x)$ denotes the gamma function. The relaxation times are summarized in Tables 3 and 4. Fitting the creep recovery gave a β value of about 0.5, whereas β reached ca. 0.7−0.9 for the relaxation of birefringence. Creep recovery became faster with increasing shear stress, according to the elastic behavior of SG-LCP-2. The relaxation time of strain recovery also decreased with increasing temperature, but the relaxation time of birefringence remained constant. Therefore, the mechanical relaxation of the backbone seemed to have no direct influence on the relaxation of the mesogenic groups.

Table 3. Relaxation Times in the Pretransitional Regime (T = 60.5 °C) as a Function of Shear Stress

σ/Pa	$\tau(\Delta n)$/s	$\tau(\gamma_{rec})$/s
200	119 ± 34	267 ± 3
300	91 ± 20	239 ± 2
400	99 ± 11	193 ± 1
500	111 ± 10	170 ± 1
590	116 ± 11	133 ± 1

Table 4. Relaxation Times in the Pretransitional Regime (σ = 500 Pa) as a Function of Temperature

temp/°C	$\tau(\Delta n)$/s	$\tau(\gamma_{rec})$/s
55.2 (nematic)	48 ± 2	187.2 ± 0.9
60.5	111 ± 10	170.7 ± 0.7
61.5	121 ± 12	145.5 ± 0.6
62.5	70 ± 15	128.9 ± 0.6
63.5	113 ± 17	117.8 ± 0.4
65.5	150 ± 48	92.5 ± 0.3

The chain length also influenced optical properties after cessation of shear. The SALS pattern relaxed to an isotropic intensity distribution, indicating that the orientation of disclination lines relaxed and the texture coarsened. The birefringence increased after cessation of shear; see Figure 7. In principal, the increase of Δn could be due to a real increase of orientation. However, one has to keep in mind that birefringence measurements can only probe the bulk orientation when the domains are sufficiently small and an average over many domains is assured.[43,44] H_v-SALS after cessation of shear showed that the depolarized scattering intensity increased at small angles and became radially isotropic. Thus, the texture coarsened and birefringence might probe a local orientation. When thicker samples were used, no increase of birefringence after cessation of shear was observed. Thus we think that the increase of Δn shown in Figure 7 was caused by insufficient averaging and additional techniques that average over larger length scales are necessary to unambiguously probe the orientation during relaxation.[44] Depolarized SALS from the low molar mass sample gave no indications for texture coarsening after cessation of shear.

In polarizing microscopy, a banded texture was observed with SG-LCP-2 after cessation of shear. Here, the sample was manually sheared between two microscope slides and the shear stress could not be controlled in this experiment. Therefore, we cannot directly correlate the banded texture with the rheo-optical experiments described above. However, the banded texture is usually related to elastic properties of the sample[45] and elastic properties were more pronounced with the high molar mass sample.

The most characteristic difference between the two samples is the **behavior of the moduli**. Figure 6 shows that the isotropic to nematic phase transition caused a decrease of G' and G'' at low frequencies for the high molar mass sample; see Figure 6. Shear alignment further decreased the moduli. Obviously, the nematic order of the mesogenic side groups affects the viscoelastic properties of the material.

The same behavior was recently observed by Rubin et al.[23] in SG-LCPs with end-on fixed mesogenic groups. In their case the mesogenic groups were oriented perpendicular to the backbone and they suggested that the nematic order dilated the confining "tube" and enhanced the mobility of the mesogens. This should

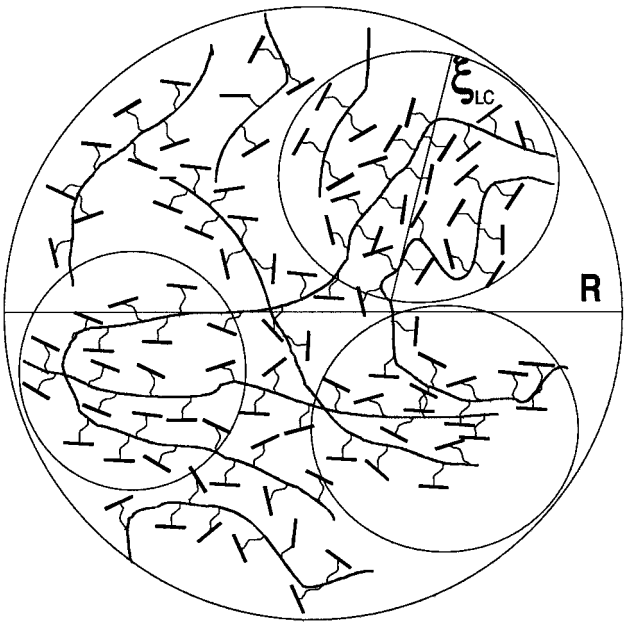

Figure 14. Schematic drawing of the chain conformation and the globular structure in the pretransitional regime.

give less hindrance to lateral fluctuations of the backbone and by that reduce the moduli.

This model, however, seems not to be transferable to our side-on SG-LCP for the following reasons: (i) The mesogenic groups were aligned in flow direction. (ii) Figure 6 indicates that the polymer chains were not entangled in our case. In contrast to Rubin et al. we did not observe a plateau modulus. Apparently, the entanglement molecular weight of our side-on SG-LCP is even higher than the values for the end-on system.

Therefore, we have to assume that the properties of the high molar mass sample cannot be interpreted with topological entanglements in a tube model. In this context we need to report some results obtained by static and dynamic light scattering in the pretransitional regime.[46]

The low molar mass sample SG-LCP-1 revealed behavior typical of low molar mass liquid crystals: the depolarized scattering intensity increased when the phase transition was approached and a critical slowing down of rotational diffusion was observed in depolarized dynamic light scattering. Both results could be interpreted with the Landau−de Gennes theory.[47]

Different behavior was found with the high molar mass sample SG-LCP-2. A strong angular dependence of scattering intensity was detected in polarized light scattering, which indicated the existence of large globular structures with a radius of ca. $r = 140$ nm. The radius decreased in the vicinity of the phase transition. The correlation length of the mesogenic swarms ξ_{LC} could be obtained from depolarized static light scattering; a schematic illustration of the structure is shown in Figure 14. A ratio of $r/\xi_{LC} \approx 2$ was found, which decreased at lower temperatures. The globular structures also gave rise to an additional slow mode in dynamic light scattering that could not be described within the framework of the Landau−de Gennes theory. Thus the interaction between mesogenic groups and the backbone seemed to be slightly unfavorable and globular structures were formed that limit possible chain configurations.

The radius of the globules and the low-frequency shear modulus decreased at the phase transition. With lowering the temperature, the interaction between the mesogens becomes more important and the interglobular repulsion decreases. As a consequence ξ_{LC} will increase in the nematic phase. Due to the long range order of the mesogens, the backbone configuration is changed, causing a shrinkage of the globular structures and less repulsive interactions. Thus, as a working hypothesis, we assume that unfavorable interactions between mesogens and the backbone become important at high molecular weight and give rise to a formation of spherical structures in the isotropic phase. In this context we wish to note that the phase transition temperature of the high molar mass sample SG-LCP-2 was lower than that of SG-LCP-1. The influence of direct mesogen interaction on structure formation has also been observed in semidilute solutions of SG-LCPs.[30] In the nematic phase interactions are dominated by the nematic field and the macroscopic alignment of domains is further increased in shear flow.

5. Conclusions

Rheo-optical properties of a side-group liquid crystalline polymer with laterally attached mesogenic groups were studied.

On the one hand, several observations indicated that rheological properties are dominated by the polymer backbone: (i) No discontinuity of viscosity at the phase transition was observed with the low molar mass sample. (ii) No or only small recoverable strains were found in recoil experiments. (iii) Rheological and optical relaxation times were different and showed different stress and temperature dependencies. Thus the behavior of the SG-LCPs with laterally attached mesogens is different as compared to main-chain LCPs.

Optically transparent, well-aligned nematic samples could be obtained for both molar masses in creep experiments. Higher order parameters were found with the low molar mass sample. Apparently, the mechanical field interacts with the texture of the nematic phase in analogy to other liquid crystalline materials. The rheological properties, however, are not dominated by the texture and an increase of molar mass reduced the birefringence.

On the other hand, the nematic order profoundly influenced storage and loss moduli of the high molar mass sample. This behavior is similar to SG-LCPs with end-on fixed mesogens. However, there are differences between side-group LCPs of side-on and end-on type, respectively.

(i) Polydomain samples of the side-on systems studied here could ***not*** be aligned by large amplitude oscillatory shear. This might be due to the fact that mesogenic groups were aligned along the flow direction.

(ii) A plateau modulus was not observed in the master curve of G' and G'', indicating that the entanglement molecular weight was not reached. Nevertheless, the isotropic to nematic phase transition influenced the moduli of the high molar mass sample. Shear orientation of the sample in the nematic state led to a further decrease of the moduli. We hypothesize that the nematic order dominated unfavorable interactions between mesogens and backbone and enhanced the mobility of the total macromolecule and by that reduced the moduli.

Acknowledgment. This work was supported by the Deutsche Forschungsgemeinschaft.

References and Notes

(1) Fuller, G. G. *Optical Rheometry of Complex Fluids*; Oxford University Press: New York, 1995.
(2) Grabowski, D. A.; Schmidt, C. *Macromolecules* **1994**, *27*, 2632.
(3) Onogi, S.; Asada, T. In *Rheology*; Astarita, G., Marrucci, G., Nicolais, G., Eds.; Plenum: New York, 1980; p 127.
(4) Marrucci, G.; Greco, F. *Adv. Chem. Phys.* **1993**, *86*, 331.
(5) Marrucci, G.; Maffetonne, P. L. In *Proceedings of the 3rd International Workshop on LCPs;* Carfanaga, C., Ed.; Pergamon Press: Oxford, U.K., 1994.
(6) Doi, M. *J. Polym. Sci., Polym. Phys. Ed.* **1981**, *19*, 229.
(7) Kwolek, S. L.; Morgan, P. W.; Schaefger, J. R.; Gukrich, L. W. *Macromolecules* **1977**, *10*, 1390.
(8) Larson, R. G.; Doi, M. *J. Rheol.* **1991**, *35*, 539.
(9) Wissbrun, K. F. *J. Rheol.* **1981**, *25*, 619.
(10) Cochini, R.; Nobile, M. R.; Acierno, D. *J. Rheol.* **1991**, *35*, 1171.
(11) Marrucci, G.; Greco, F. In *Advances in Chemistry Physics;* Prigogine, I, Rice, S. A., Eds.; John Wiley & Sons, Inc.: New York, 1993; Vol. 86.
(12) Moldenaers, P. In *Liquid Crystalline Polymers*; Acierno, D., Collyer, A. A., Eds.; Chapman & Hall: London, 1996.
(13) Walker, L. M.; Wagner, N. *J. Rheol.* **1994**, *38*, 1525.
(14) Mewis, J.; Mortier, M.; Vermant, J.; Moldenaers, P. *Macromolecules* **1997**, *30*, 1323.
(15) Zentel, R.; Wu, J. *Makromol. Chem.* **1986**, *187*, 1727.
(16) Colby, R. H.; Gillmore, J. R.; Galli, G.; Laus, M.; Ober, C. K.; Hall, E. *Liq. Cryst.* **1993**, *13*, 233.
(17) Zhao, Y.; Roche, P.; Yuan, G. *Macromolecules* **1996**, *29*, 4619.
(18) Götz, S.; Stille, W.; Strobl, G.; Scheuermann, H. *Macromolecules* **1993**, *26*, 1520.
(19) Siebert, H.; Grabowski, D. A.; Schmidt, C. Submitted to *Rheol. Acta*.
(20) Wissbrunn, K. F.; Griffin, A. C. *J. Polym. Sci., Polym. Phys. Ed.* **1982**, *20*, 1835.
(21) Kannan, R. M.; Kornfield, J. A.; Schwenk N.; Boeffel, C. *Macromolecules* **1993**, *26*, 2050.
(22) McArdle, C. M., Ed. *Side Chain Liquid Crystal Polymers;* Blackie and Son Ltd.: Glasgow, 1989.
(23) Rubin, S. F.; Kannan, R. M.; Kornfield, J. A.; Boeffel, C. *Macromolecules* **1995**, *28*, 3521.
(24) Hessel, F.; Finkelmann, H. *Makromol. Chem.* **1988**, *189*, 2275.
(25) Hessel, F.; Herr, R. P.; Finkelmann, H. *Makromol. Chem.* **1987**, *188*, 1597.
(26) Schätzle, J.; Kaufhold, W.; Finkelmann, H. *Makromol. Chem.* **1989**, *190*, 3269.
(27) Lecommandoux, S.; Noirez, L.; Richard, H.; Achard, M. F.; Strazielle, C.; Hardouin, F. *J. Phys. II Fr.* **1996**, *6*, 225.
(28) Lim, K.-C.; Ho, J. T. *Mol. Cryst. Liq. Cryst.* **1978**, *47*, 173.
(29) Schmidt, J.; Weigel, R.; Burchard, W.; Richtering, W. *Macromol. Symp.* **1997**, *120*, 247.
(30) Richtering, W.; Gleim, W.; Burchard, W. *Macromolecules* **1992**, *25*, 3795.
(31) Warner, M.; Wang, X. J. *Macromolecules* **1991**, *24*, 4932.
(32) Porter, R. S.; Johnson, J. F. *Rheology*, Eirich, F. R., Ed.; Academic Press, New York, 1967.
(33) Larson, R. G.; Mead, D. W. *J. Rheol.* **1989**, *33*, 1251.
(34) Hessel, F. Ph.D. Thesis, University of Freiburg, Germany, 1987.
(35) Picken, S. J.; Aerts, J.; Doppert, H. L.; Reuvers, A. J.; Norholt, M. G. *Macromolecules* **1991**, *24*, 1366.
(36) Patlazhan, S. A.; Riti, J. B.; Navard, P. *Macromolecules* **1996**, *29*, 2029.
(37) Vermant, J. Ph.D. Thesis, Department Chemical Engineering, K. U. Leuven, Belgium, 1996.
(38) Moldenaers, P.; Mewis, J. *J. Non-Newtonian Fluid Mech.* **1990**, *34*, 359.
(39) Laun, H. M. *J. Rheol.* **1986**, *33*, 459.
(40) Kohlrausch, R. *Ann. Phys.* **1847**, *12*, 393.
(41) Williams, G.; Watts, D. C. *Trans. Faraday Soc.* **1970**, *66*, 80.
(42) Lindsey, C. P.; Patterson, G. D. *J. Chem. Phys.* **1980**, *73*, 3348.
(43) Hongladarom, K.; Burghardt, W. R. *Macromolecules* **1993**, *26*, 785.
(44) Hongladarom, K.; Ugaz, V. M.; Cinader, D. K.; Burghardt, W. R.; Quintana, J. P.; Hsiao, B. S.; Dadmun, M. D.; Hamilton, W. A.; Butler, P. D. *Macromolecules* **1996**, *29*, 5346.
(45) Navard, P.; Zachariades, A. E. *J. Polym. Sci., Polym. Phys. Ed.* **1987**, *25*, 1089.
(46) Fuchs, J. Ph.D. Thesis, University of Freiburg, Germany, 1996.
(47) de Gennes, P. G. *The Physics of Liquid Crystals*; Clarendon Press, Oxford, U.K., 1974.

MA970430I